

# Supporting Information

## Template-Oriented Synthesis of Nitrogen-Enriched Porous Carbon Nanowhisker by Hollow TiO<sub>2</sub> Spheres Nanothorns for Methanol Electrooxidation

Jun Zhang,<sup>\*†</sup> Xiaoyan Liu,<sup>†</sup> An Xing,<sup>†</sup> Juan Liu<sup>\*‡</sup>

<sup>†</sup>School of Metallurgy and Materials Engineering, Chongqing Key Laboratory of Nano/Micro Composites and Devices, Chongqing University of Science & Technology, Chongqing 401331, China

<sup>‡</sup>College of Chemistry and Chemical Engineering, Chongqing University of Science & Technology, Chongqing 401331, China

\* (J.Z.) E-mail: 2017003@cqust.edu.cn

\*(J.L.) E-mail: ljyxj@126.com

## Detailed Experimental Procedures

### Materials

Isopropyl titanate, polyvinylpyrrolidone (PVP), aniline (An), ammonium peroxydisulfate (APS), sulfuric acid, methanol, ethylene glycol (EG) were all purchased from Chuandong Chemical Reagent Company (Chengdu, China). Chloroplatinic acid hexahydrate ( $\text{H}_2\text{PtCl}_6 \cdot 6\text{H}_2\text{O}$ , 99.9%) was obtained from the First Reagent Factory (Shanghai, China).  $\text{SiO}_2$  with the particle size of 15 nm was brought from Aladdin (Shanghai, China). Nafion solution (5 wt%) was gained from Dupont China Holding Co., Ltd. Ultrapure water (Millipore, 18.2 M $\Omega$  cm) was used throughout all experiments. All other reagents were of analytical grade and used without further purification.

### Synthesis of H-TiO<sub>2</sub> spheres

Typically, the method was described in a previous publication.<sup>1</sup> In brief, 0.84 mL of ammonia and 1.82 mL of ultrapure water were added into a mixed solution that contained 300 mL ethanol and 200 mL acetonitrile. 10 mL isopropyl titanate was then quickly injected into the above solution with vigorous stirring for 6 h followed by filtration and rinsed with ethanol. Subsequently, 0.67 g TiO<sub>2</sub> sphere was dispersed in 13.3 mL of ultrapure water and kept for ultrasound about 2 h. After that, 0.058 g of NaF (etching agents) was added and stirred for another 1 h, and then 0.067 g of PVP was sequentially added. After stirring for another 1 h, the mixed solution was transferred into 20 mL autoclave and heated to 110 °C for 4 h to conduct the crystallization and targeted etching process. The final H-TiO<sub>2</sub> samples were calcined at a heating rate of 1 °C min<sup>-1</sup> at 350 °C for 2 h.

### Synthesis of H-TiO<sub>2</sub>@N-HPCN supports

0.45 g of H-TiO<sub>2</sub> with 1.6 g PVP was added into 100 mL of ultrapure water and continuously stirred at 100 °C for 4 h to obtain PVP surface modified H-TiO<sub>2</sub> spheres (H-TiO<sub>2</sub>/PVP). Then 0.3 g SiO<sub>2</sub> NPs was taken in 20 mL of ultrapure water at 100 °C for 2 h to generate a high coverage of hydroxyl groups. Subsequently, 0.685 mL of aniline and 0.226 g of SiO<sub>2</sub> NPs were dispersed in 100 mL 1 M H<sub>2</sub>SO<sub>4</sub> solution followed by 0.5 h of sonication, and then 0.4 g of H-TiO<sub>2</sub>/PVP was added. After stirring for 12 h, 100 mL 1 M H<sub>2</sub>SO<sub>4</sub> solutions containing 1.72 g of APS were slowly dropwise added into the mixed solutions within 3 h and further stirring at 0 °C for 12 h to obtain H-TiO<sub>2</sub>@PANI/SiO<sub>2</sub> nanowhisker. The desired product was collected by centrifuging and washed with ethanol and then dried at 60 °C. Finally, the H-TiO<sub>2</sub>@PANI/SiO<sub>2</sub> nanowhisker was annealed from temperature to 700, 800, or 900 °C with a 5 °C min<sup>-1</sup> heating rate under N<sub>2</sub> atmosphere, and then kept for 2 h to obtain nitrogen-enriched porous carbon nanowhisker (N-PCN) and SiO<sub>2</sub> NPs coated hollow TiO<sub>2</sub> sphere (H-TiO<sub>2</sub>@N-PCN/SiO<sub>2</sub>-T, T=700, 800 and 900). After removal of SiO<sub>2</sub> NPs in 2 M HF + 8 M NH<sub>4</sub>F aqueous solutions, the obtained materials were marked as H-TiO<sub>2</sub>@N-HPCN-T (T=700, 800 and 900).

### Synthesis of Pt/H-TiO<sub>2</sub>@N-HPCN catalysts

Pt/H-TiO<sub>2</sub>@N-HPCN catalysts with a nominal Pt loading of 20 wt% were prepared by using microwave-assisted polyol process. Generally, 20 mg of H-TiO<sub>2</sub>@N-HPCN was suspended into a mixture solvent containing 12 mL of EG and 3 mL of isopropanol by sonication for 1 h. Then, 0.684 mL of 0.03746 M H<sub>2</sub>PtCl<sub>6</sub>-EG solution was injected with urgent agitation for 3 h. After adjusting the pH value to 12 by adding 1 M NaOH-EG solution and then being saturated with N<sub>2</sub>, the suspension was heated in microwave reactor (2450 MHz, 800 W) for 60 s. Eventually, the pH value of the resultant mixture was adjusted to 3 with 0.1 M HNO<sub>3</sub> solution and then constantly stirring for 12 h. The desired catalysts were denoted as Pt/H-TiO<sub>2</sub>@N-HPCN-T (700, 800 and 900). Commercial Pt/C (E-TEK) catalyst (3.3 nm, 20 wt% Pt supported on Vulcan XC-72R carbon) was used for comparison.

### Materials characterization

The crystal structure was performed on a X-ray powder diffraction (XRD, PANalytical X' Pert Powder) using Cu-K $\alpha$  radiation. The Fourier transform infrared (FTIR) spectra were recorded with a ThermoFisher NICOLET iS50 FTIR spectrometer. Composition was carried out on an inductively coupled plasma optical emission spectrometry (ICP, iCAP 6300 Duo). Catalyst structure was performed by using Transmission electron microscopy (TEM), high-resolution TEM (HRTEM) on a Zeiss LIBRA 200 microscope operating at 200 kV, the morphology of all samples was studied by a scanning

electron microscopy (SEM) on a Hitachi S-4800 electron microscope. X-ray photoelectron spectroscopy (XPS) analysis was taken by an ESCALAB 250 system from a monochromator Al K $\alpha$  X-ray source (1486.7 eV) to determine the surface property of the samples. Brunauer-Emmett-Teller (BET) surface area of the samples was measured by nitrogen adsorption-desorption on a QUADRASORB SI Automated Surface Area & Pore Size Analyzer.

### Electrochemical measurements

Cyclic voltammetry (CV) and chronoamperometric (CA) were carried on a CHI 660d electrochemical workstation (Chenhua Co., Shanghai, China). A standard three-electrode system was used with a saturated calomel electrode (SCE) as a reference electrode, Pt foil as a counter electrode, and glassy carbon electrode (GCE, 5 mm in diameter) as a working electrode. All potentials reported herein were versus the SCE. To investigate the electrochemical performance, 2.0 mg catalyst was first mixed up with a solution composed of 0.4 mL of ethanol and 10  $\mu$ L of Nafion solution (5.0 wt%), and then sonicated for 0.5 h to form a homogeneous catalyst ink, subsequently, a total of 10  $\mu$ L of as-prepared ink was dropped onto a prepolished GCE and dried at room temperature. To evaluate the tolerance of the catalyst against CO poisoning, the 0.5 M H<sub>2</sub>SO<sub>4</sub> solution was bubbled with CO gas for 20 min at 0.1 V, followed by bubbling with N<sub>2</sub> gas for 20 min to remove residual CO in solution. Then, CO stripping voltammetry was measured between -0.2 and 0.95 V at a scan rate of 10 mV s<sup>-1</sup>. The electrochemically active surface area (ECSA) was measured using the CO oxidation charge after subtracting the base current of the subsequent CV curve, by assuming 420  $\mu$ C cm<sup>-2</sup> as the oxidation charge for one monolayer of CO on a smooth Pt surface.<sup>2</sup> The MOR was examined in 0.5 M H<sub>2</sub>SO<sub>4</sub> + 1.0 M CH<sub>3</sub>OH solutions between -0.2 and 0.95 V with a scan rate of 50 mV s<sup>-1</sup>. The accelerated CV test was firstly performed for 1000 cycles with a scan rate of 200 mV s<sup>-1</sup> in 0.5 M H<sub>2</sub>SO<sub>4</sub> + 1.0 M CH<sub>3</sub>OH solutions, and subsequently the fresh electrolyte solution was used to measure new CV curves with a scan rate of 50 mV s<sup>-1</sup>. Chronoamperometry (CA) tests were performed for 3600 s at 0.65 V to further investigate the long-term durability. All of the used electrolytes were saturated with ultrapure N<sub>2</sub> gas for nearly 30 min to remove dissolved oxygen before starting measurements.

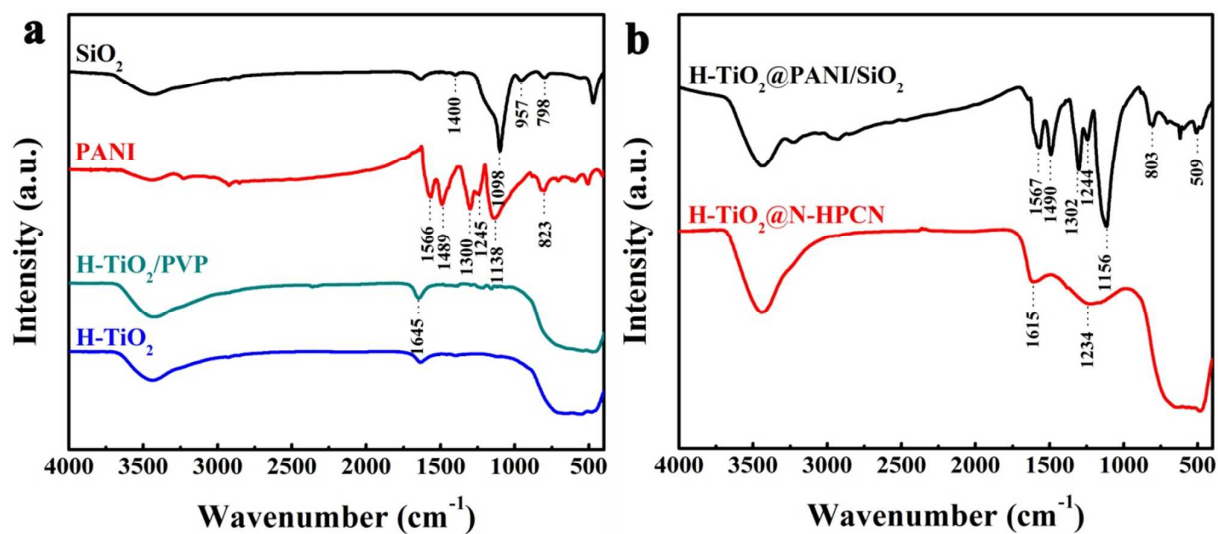


Figure S1 FTIR spectra of (a) H-TiO<sub>2</sub>, H-TiO<sub>2</sub>/PVP, SiO<sub>2</sub> and PANI, (b) H-TiO<sub>2</sub>@PANI/SiO<sub>2</sub> and H-TiO<sub>2</sub>@N-HPCN-800.

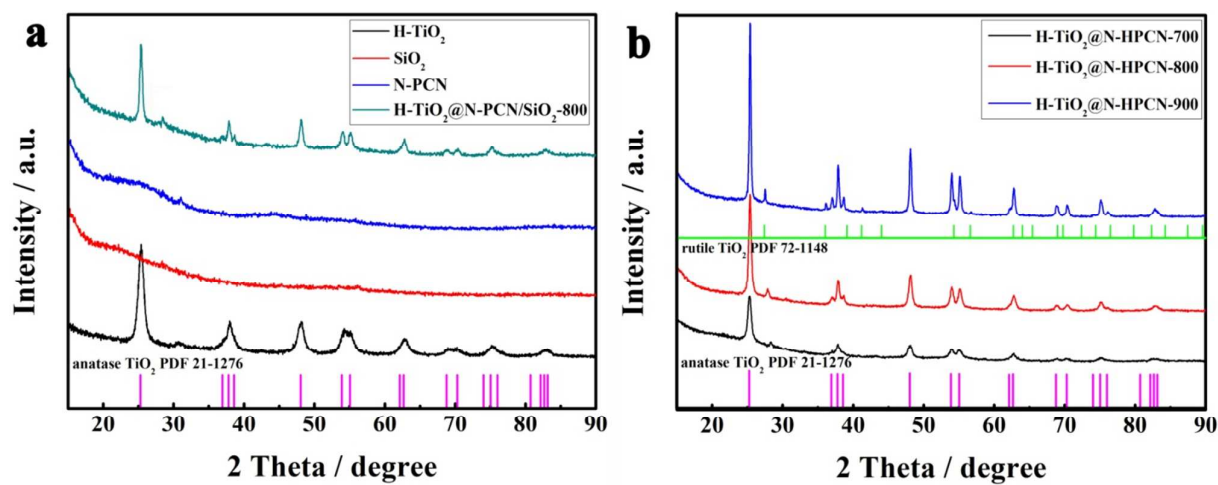
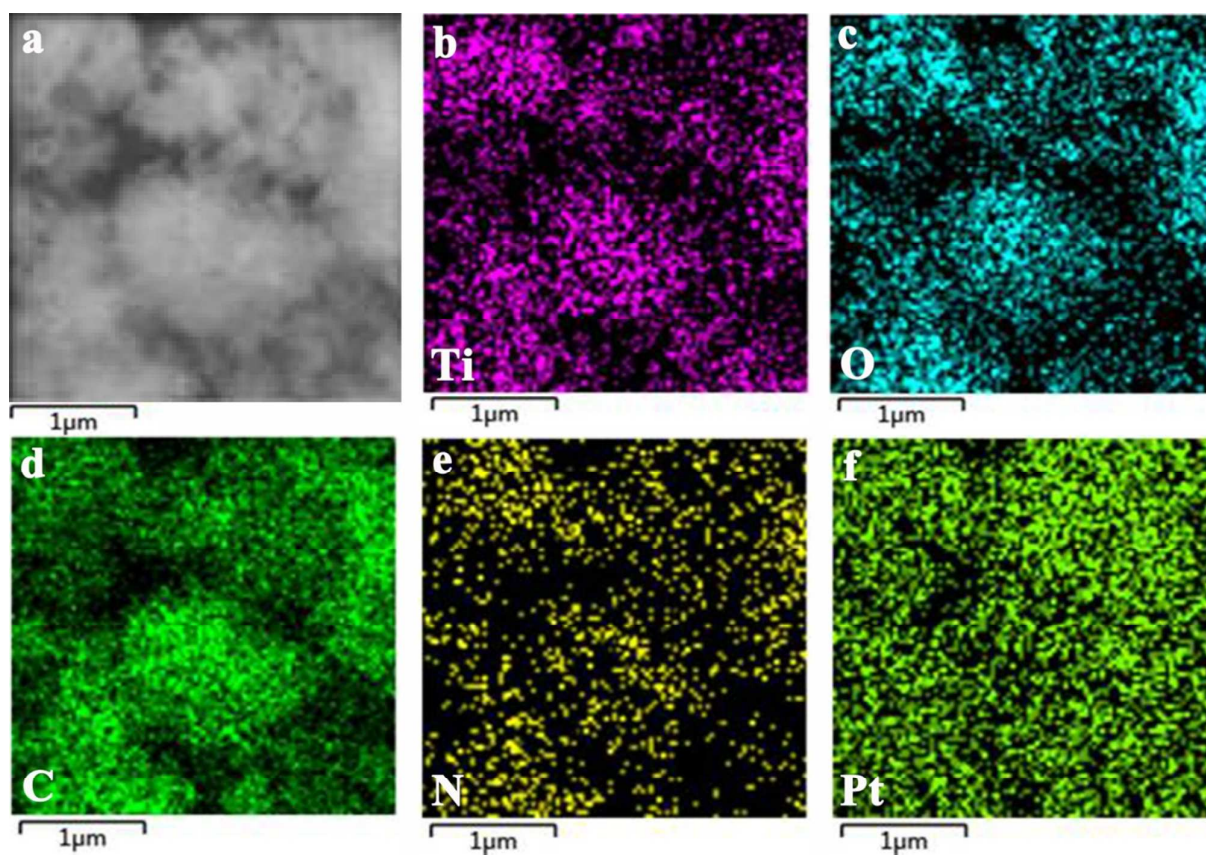
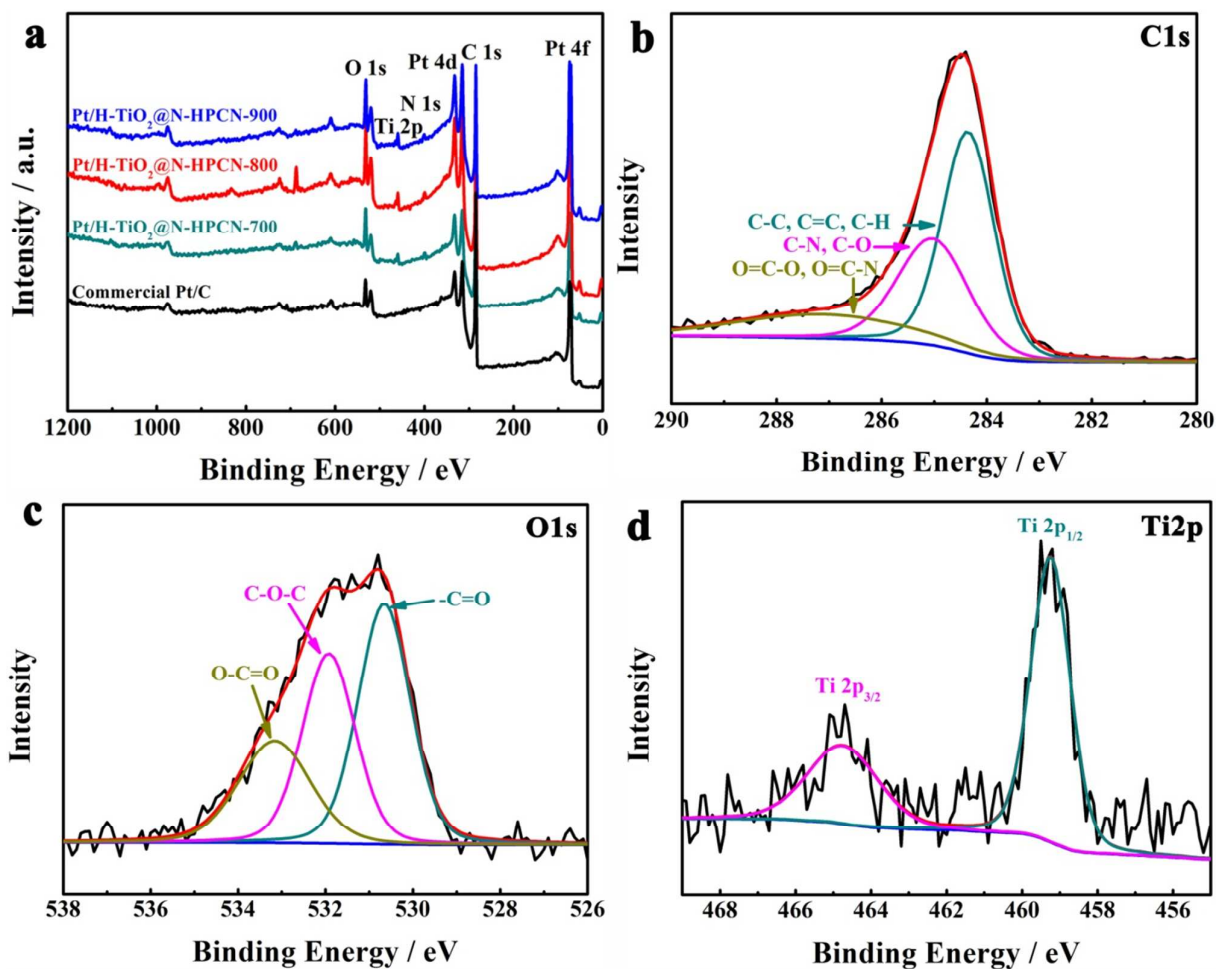


Figure S2 XRD patterns of (a) H-TiO<sub>2</sub>, SiO<sub>2</sub>, N-PCN-800, H-TiO<sub>2</sub>@N-PCN/SiO<sub>2</sub>-800, (b) H-TiO<sub>2</sub>@N-HPCN-T (T=700, 800 and 900).



**Figure S3** (a) SEM images of the Pt/H-TiO<sub>2</sub>@N-HPCN-800 catalyst and corresponding elemental mapping of (b) Ti, (c) O, (d) C, (e) N, and (f) Pt.



**Figure S4** XPS survey spectra (a) of Pt/H-TiO<sub>2</sub>@N-HPCN-T (T=700, 800 and 900) and commercial Pt/C. High resolution (b) C 1s, (c) O 1s, and (d) Ti 2p XPS spectra of the Pt/H-TiO<sub>2</sub>@N-HPCN-800.

**Table S1** Chemical composition of Pt/H-TiO<sub>2</sub>@N-HPCN-T (T=700, 800 and 900) and commercial Pt/C catalysts obtained by XPS analysis.

Samples	C (at.%)	N (at.%)	Ti (at.%)	O (at.%)	Pt (at.%)
Pt/H-TiO <sub>2</sub> @N-HPCN-700	75.30	3.24	1.38	14.24	5.84
Pt/H-TiO <sub>2</sub> @N-HPCN-800	69.10	3.77	0.64	15.77	10.73
Pt/H-TiO <sub>2</sub> @N-HPCN-900	73.46	1.02	2.05	13.80	9.67
Commercial Pt/C	85.51	-	-	8.26	6.23

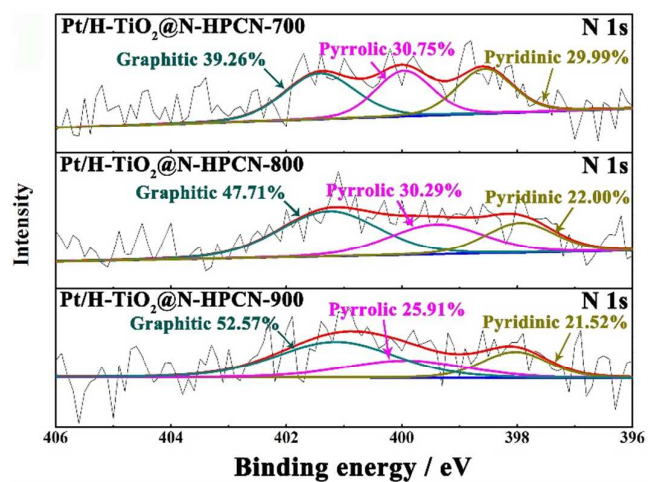


**Figure S5** N 1s High resolution XPS of Pt/H-TiO<sub>2</sub>@N-HPCN-T (T=700, 800 and 900) catalysts.

**Table S2** Comparison of the positive scan peak current density normalized as mass activity for the Pt/H-TiO<sub>2</sub>@N-HPCN-800 catalyst and other recently reported catalysts.

Catalyst	Mass activity (A mg <sup>-1</sup> )	Scanning	Condition	Ref.
		rate (mV s <sup>-1</sup> )		
Pt/TiO <sub>2</sub> @N-doped C-900	0.490	50	0.5 M H <sub>2</sub> SO <sub>4</sub> + 1.0 M CH <sub>3</sub> OH	<sup>3</sup>
Pt/TiO <sub>2</sub> @NCX-900	0.354	50	0.5 M H <sub>2</sub> SO <sub>4</sub> + 1.0 M CH <sub>3</sub> OH	<sup>4</sup>
Pt/NCX-TiO <sub>2</sub> -2	0.382	50	0.5 M H <sub>2</sub> SO <sub>4</sub> + 1.0 M CH <sub>3</sub> OH	<sup>5</sup>
Pt/TiO <sub>2</sub> @C-900	0.155	50	0.5 M H <sub>2</sub> SO <sub>4</sub> + 2.0 M CH <sub>3</sub> OH	<sup>6</sup>
Pt/TiO <sub>2</sub> /G	0.254	50	0.5 M H <sub>2</sub> SO <sub>4</sub> + 1.0 M CH <sub>3</sub> OH	<sup>7</sup>
Pt/TiO <sub>2</sub> -C	0.103	50	0.5 M H <sub>2</sub> SO <sub>4</sub> + 0.5 M CH <sub>3</sub> OH	<sup>8</sup>
Pt/C-TNTs	ca. 0.350	50	0.5 M H <sub>2</sub> SO <sub>4</sub> + 0.5 M CH <sub>3</sub> OH	<sup>9</sup>
Pt-PANI/TiO <sub>2</sub> -C	0.640	50	0.5 M H <sub>2</sub> SO <sub>4</sub> + 0.5 M CH <sub>3</sub> OH	<sup>10</sup>
Pt/C-TNTs-EG	0.450	50	0.5 M H <sub>2</sub> SO <sub>4</sub> + 0.5 M CH <sub>3</sub> OH	<sup>11</sup>
Pt/C-HTNTs-7	0.530	50	0.5 M H <sub>2</sub> SO <sub>4</sub> + 0.5 M CH <sub>3</sub> OH	<sup>12</sup>
Pt/C-STNS-600	0.480	50	0.5 M H <sub>2</sub> SO <sub>4</sub> + 0.5 M CH <sub>3</sub> OH	<sup>13</sup>
G-P-G	0.463	50	0.5 M H <sub>2</sub> SO <sub>4</sub> + 0.5 M CH <sub>3</sub> OH	<sup>14</sup>
Pt-WO <sub>2</sub> /WO <sub>3</sub>	0.694	50	0.5 M H <sub>2</sub> SO <sub>4</sub> + 1.0 M CH <sub>3</sub> OH	<sup>15</sup>
Pt@Heli-CeO <sub>2</sub> /C	ca. 0.670	50	0.5 M H <sub>2</sub> SO <sub>4</sub> + 2.0 M CH <sub>3</sub> OH	<sup>16</sup>
Pt/CeO <sub>2</sub> -15μL	0.288	20	0.5 M H <sub>2</sub> SO <sub>4</sub> + 0.5 M CH <sub>3</sub> OH	<sup>17</sup>
Pt/TiN@NDC	0.626	50	0.1 M HClO <sub>4</sub> + 1.0 M CH <sub>3</sub> OH	<sup>18</sup>
Pt/TiN-G	0.252	20	0.5 M H <sub>2</sub> SO <sub>4</sub> + 0.5 M CH <sub>3</sub> OH	<sup>19</sup>
Pd/PRGO	1.112	50	0.5 M H <sub>2</sub> SO <sub>4</sub> + 1.0 M HCOOH	<sup>20</sup>
Pd/HHTTS	0.362	50	0.5 M H <sub>2</sub> SO <sub>4</sub> + 1.0 M HCOOH	<sup>21</sup>
Pt/GR-CNTs	0.550	50	0.5 M H <sub>2</sub> SO <sub>4</sub> + 1.0 M CH <sub>3</sub> OH	<sup>22</sup>
Pt/H-TiO <sub>2</sub> @N-HPCN-800	0.695	50	0.5 M H <sub>2</sub> SO <sub>4</sub> + 1.0 M CH <sub>3</sub> OH	This work



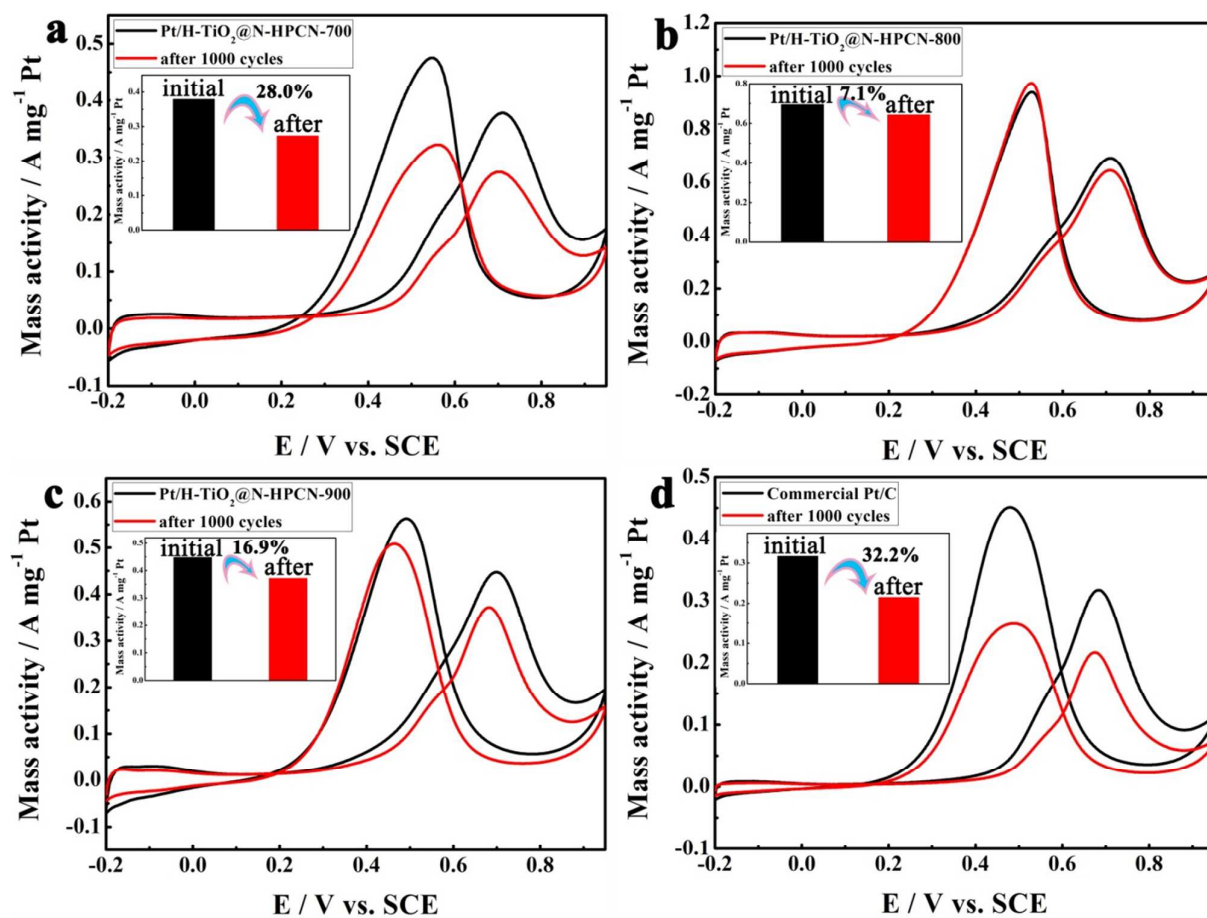


**Figure S6** (a-d) Cyclic voltammograms of Pt/H-TiO<sub>2</sub>@N-HPCN-T (T=700, 800 and 900) and commercial Pt/C catalysts in 0.5 M H<sub>2</sub>SO<sub>4</sub> + 1.0 M CH<sub>3</sub>OH solutions at a scan rate of 50 mV s<sup>-1</sup>.

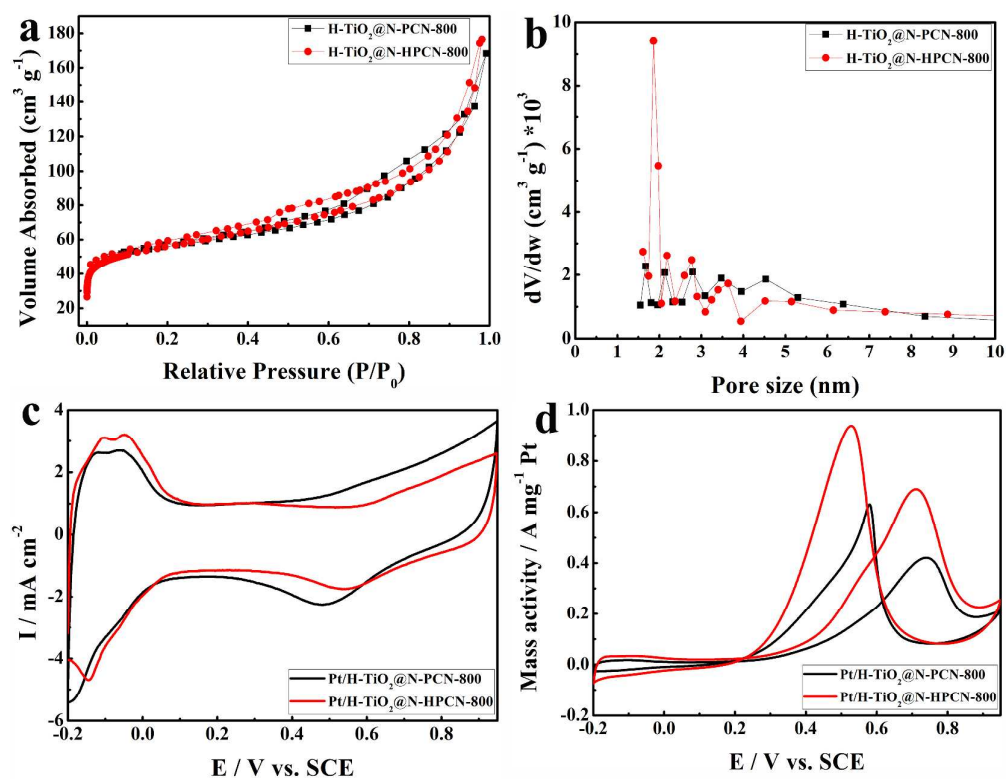


**Figure S7** N<sub>2</sub> absorption-desorption isotherm (a) and pore size distribution (b) of  $\text{H-TiO}_2\text{@N-PCN-800}$  and  $\text{H-TiO}_2\text{@N-HPCN-800}$ ; CVs of the  $\text{Pt/H-TiO}_2\text{@N-PCN-800}$  and  $\text{Pt/H-TiO}_2\text{@N-HPCN-800}$  catalysts in deaerated 0.5 M  $\text{H}_2\text{SO}_4$  solution (c) and in a solution of 0.5 M  $\text{H}_2\text{SO}_4$  + 1.0 M  $\text{CH}_3\text{OH}$  (d).

## Reference

- (1) Pan, J. H.; Wang, X. Z.; Huang, Q.; Shen, C.; Koh, Z. Y.; Wang, Q.; Engel, A.; Bahnemann, D. W. Large-scale Synthesis of Urchin-like Mesoporous TiO<sub>2</sub> Hollow Spheres by Targeted Etching and Their Photoelectrochemical Properties. *Adv. Funct. Mater.* **2014**, *24*, 95-104.
- (2) Ting, C.-C.; Liu, C.-H.; Tai, C.-Y.; Hsu, S.-C.; Chao, C.-S.; Pan, F.-M. The size effect of titania-supported Pt nanoparticles on the electrocatalytic activity towards methanol oxidation reaction primarily via the bifunctional mechanism. *J. Power Sources* **2015**, *280*, 166-172.
- (3) Zhao, X.; Zhu, J.; Liang, L.; Liao, J.; Liu, C.; Xing, W. Enhanced activity of Pt nano-crystals supported on a novel TiO<sub>2</sub>@N-doped C nano-composite for methanol oxidation reaction. *J. Mater. Chem.* **2012**, *22*, 19718-19725.
- (4) Zhu, J.; Xiao, M.; Zhao, X.; Liu, C.; Xing, W. Titanium dioxide encapsulated in nitrogen-doped carbon enhances the activity and durability of platinum catalyst for Methanol electro-oxidation reaction. *J. Power Sources* **2015**, *292*, 78-86.
- (5) Zhu, J.; Zhao, X.; Xiao, M.; Liang, L.; Liu, C.; Liao, J.; Xing, W. The construction of nitrogen-doped graphitized carbon-TiO<sub>2</sub> composite to improve the electrocatalyst for methanol oxidation. *Carbon* **2014**, *72*, 114-124.
- (6) Lee, J.-M.; Han, S.-B.; Kim, J.-Y.; Lee, Y.-W.; Ko, A. R.; Roh, B.; Hwang, I.; Park, K.-W. TiO<sub>2</sub>@carbon core-shell nanostructure supports for platinum and their use for methanol electrooxidation. *Carbon* **2010**, *48*, 2290-2296.
- (7) Hua, H.; Hu, C.; Zhao, Z.; Liu, H.; Xie, X.; Xi, Y. Pt nanoparticles supported on submicrometer-sized TiO<sub>2</sub> spheres for effective methanol and ethanol oxidation. *Electrochim. Acta* **2013**, *105*, 130-136.
- (8) Fan, Y.; Yang, Z.; Huang, P.; Zhang, X.; Liu, Y.-M. Pt/TiO<sub>2</sub>-C with hetero interfaces as enhanced catalyst for methanol electrooxidation. *Electrochim. Acta* **2013**, *105*, 157-161.
- (9) Sui, X.-L.; Wang, Z.-B.; Yang, M.; Huo, L.; Gu, D.-M.; Yin, G.-P. Investigation on C-TiO<sub>2</sub> nanotubes composite as Pt catalyst support for methanol electrooxidation. *J. Power Sources* **2014**, *255*, 43-51.
- (10) Yang, F.; Ma, L.; Gan, M.; Zhang, J.; Yan, J.; Huang, H.; Yu, L.; Li, Y.; Ge, C.; Hu, H. Polyaniline-functionalized TiO<sub>2</sub>-C supported Pt catalyst for methanol electro-oxidation. *Synth. Met.* **2015**, *205*, 23-31.
- (11) Sui, X.-L.; Wang, Z.-B.; Xia, Y.-F.; Yang, M.; Zhao, L.; Gu, D.-M. A rapid synthesis of TiO<sub>2</sub> nanotubes in an ethylene glycol system by anodization as a Pt-based catalyst support for methanol electrooxidation. *RSC Adv.* **2015**, *5*, 35518-35523.
- (12) Sui, X.-L.; Wang, Z.-B.; Li, C.-Z.; Zhang, J.-J.; Zhao, L.; Gu, D.-M. Effect of pH value on H<sub>2</sub>Ti<sub>2</sub>O<sub>5</sub>/TiO<sub>2</sub> composite nanotubes as Pt catalyst support for methanol oxidation. *J. Power Sources* **2014**, *272*, 196-202.
- (13) Sui, X.-L.; Wang, Z.-B.; Li, C.-Z.; Zhang, J.-J.; Zhao, L.; Gu, D.-M.; Gu, S. Multiphase sodium titanate/titania composite nanostructures as Pt-based catalyst supports for methanol oxidation. *J. Mater. Chem. A* **2015**, *3*, 840-846.
- (14) Zhao, L.; Wang, Z.-B.; Li, J.-L.; Zhang, J.-J.; Sui, X.-L.; Zhang, L.-M. A newly-designed sandwich-structured graphene-Pt-graphene catalyst with improved electrocatalytic performance for fuel cells. *J. Mater. Chem. A* **2015**, *3*, 5313-5320.
- (15) Zhou, Y.; Hu, X.-C.; Liu, X.-H.; Wen, H.-R. Core-shell hierarchical WO<sub>2</sub>/WO<sub>3</sub> microspheres as an electrocatalyst support for methanol electrooxidation. *Chem. Commun.* **2015**, *51*, 15297-15299.
- (16) Chen, J.; Li, S.; Du, J.; Liu, J.; Yu, M.; Meng, S.; Wang, B. Superior methanol electrooxidation activity and CO tolerance of mesoporous helical nanospindle-like CeO<sub>2</sub> modified Pt/C. *RSC Adv.* **2015**, *5*, 64261-64267.
- (17) Chu, Y. Y.; Cao, J.; Dai, Z.; Tan, X. Y. A novel Pt/CeO<sub>2</sub> catalyst coated with nitrogen-doped carbon with excellent performance for DMFCs. *J. Mater. Chem. A* **2014**, *2*, 4038-4044.
- (18) Zhang, J.; Ma, L.; Gan, M.; Fu, S.; Zhao, Y. TiN@nitrogen-doped carbon supported Pt nanoparticles as high-performance anode catalyst for methanol electrooxidation. *J. Power Sources* **2016**, *324*, 199-207.
- (19) Qi, L.; Yin, Y.; Shi, W.; Liu, J.; Xing, D.; Liu, F.; Hou, Z.; Gu, J.; Ming, P.; Zou, Z. Intermittent microwave synthesis of nanostructured Pt/TiN-graphene with high catalytic activity for methanol oxidation. *Int. J. Hydrogen Energy* **2014**, *39*, 16036-16042.
- (20) Zhou, Y.; Hu, X.-C.; Fan, Q.; Wen, H.-R. Three-dimensional crumpled graphene as an electro-catalyst support for formic acid electro-oxidation. *J. Mater. Chem. A* **2016**, *4*, 4587-4591.

- (21) Hu, X.; Zhou, Y.; Wen, H.; Zhong, H. Hierarchical Hollow Tungsten Trioxide Sphere as an Electrocatalyst Support for Formic Acid Electrooxidation. *J. Electrochem. Soc.* **2014**, *161*, F583-F587.
- (22) Zhou, Y.; Hu, X.; Guo, S.; Yu, C.; Zhong, S.; Liu, X. Multi-functional graphene/carbon nanotube aerogels for its applications in supercapacitor and direct methanol fuel cell. *Electrochim. Acta* **2018**, *264*, 12-19.